RevMexAA (Serie de Conferencias), **1**, 85-91 (1995)

OUTFLOWS AND WATER MASERS IN STAR-FORMING REGIONS

Moshe Elitzur
Department of Physics and Astronomy
University of Kentucky, Lexington KY 40506, USA

RESUMEN

La emisión intensa de máser de agua es un indicador importante del proceso de formación estelar, pudiendo trazar las últimas etapas de evolución antes de que emerja una estrella masiva. Los choques con velocidades $\gtrsim 20$ km s^{-1} contra material magnetizado de alta densidad ($\gtrsim 3\times10^6$ cm^{-3}) explican de una forma satisfactoria esa emisión máser. Observaciones de los máseres en W49 y W3OH, realizadas recientemente, muestran que éstos se encuentran en las superficies de cascarones alargados, expandiéndose por la acción de chorros gemelos muy jóvenes (unos cuantos cientos de años) y con una gran velocidad ($\sim$ 1000 km s^{-1}). Los tiempos de escala que se estiman para esos máseres de H_2O parecen ser muy cortos ($\lesssim$ 2000 años).

ABSTRACT

Powerful water maser emission is an important signpost of the star formation process, and may delineate the very last stages before the emergence of a high-mass star. Shocks with velocities $\gtrsim 20$ km s^{-1} running into high-density ($\gtrsim 3\times10^6$ cm^{-3}) magnetized material successfully explain the maser emission. Recent high-resolution observations of the masers in W49 and W3OH show that the maser features outline the surfaces of elongated cocoons whose expansion is driven by twin high-velocity ($\sim$ 1000 km s^{-1}), very young (a few hundred years) jets. Short time scales ($\lesssim$ 2000 years) for any given H_2O maser seem unavoidable.

Key words: **MASERS — ISM: JETS AND OUTFLOWS — STARS: FORMATION — STARS: PRE-MAIN-SEQUENCE**

1. INTRODUCTION

Strong H_2O maser emission is a prominent signpost of star formation. Water masers are found in all classes of star-forming regions, where they are virtually always associated with outflows whose velocities range from $\sim$ 20 km s^{-1} to $\sim$ 200 km s^{-1}. Weaker masers occur in low-mass star forming regions, where they are associated with T Tauri, or other pre-main sequence, stars. The more powerful masers are found in high-mass star forming regions, where the evolutionary stage and the nature of the star(s) responsible for exciting the masers are largely unknown. While maser emission is widespread, there is also a high degree of selectivity associated with this phase of star formation. A case in point is W49. High resolution observations by Welch et al. (1987) show that the core of this star-forming region contains at least ten distinct ultra-compact HII regions arranged in a ring-like structure with a diameter of 2 pc. Only one of these objects is also a water maser, by far the most powerful maser in the Galaxy. Although the brightest, there are no distinct observed properties that set this object apart from others in the ring to indicate why they currently are not detected in H_2O maser emission.

Because masers probe small-scale structure and fine details, progress in their understanding has been strongly tied to advances in high-resolution observations. The rapid advances in interferometric capabilities of the past few years have led to important clues to the nature of the H_2O maser phase, and a coherent picture is beginning to emerge.

2. BASIC MODEL FOR MASER ACTION

Proper motion experiments conclusively show that the highly supersonic velocities recorded in maser spectra reflect true space velocities. Maser features are actually moving across the sky at these high velocities, invariably associated with powerful shocks. Elitzur, Hollenbach, & McKee (1989, 1992) show that shocks propagating in high-density ($n_0 \gtrsim 3\times10^6$ cm^{-3}), magnetized regions provide a natural environment for H_2O maser action. The shocked material has both the high temperature ($\sim$ 400 K) and high density ($\sim 10^9$ cm^{-3}) required to collisionally excite the maser levels, as well as the high H_2O abundance ($\sim 10^{-5}$) necessary for powerful maser action. Equally important is the planar, slab-like geometry which enables thermal photons to escape through the slab's faces, avoiding thermalization. Strong maser radiation is generated for propagation in the plane, leading to an inverse variation of maser intensity with Doppler velocity, as observed. An important result is that the maser geometrical shape in the plane of the slab is largely irrelevant. The only relevant property is the maser length along the line of sight — a disk and a cylinder for which these lengths are equal have comparable brightness. This length is set by the requirement of velocity coherence along the line of sight and is controlled either by the local turbulence field or by the curvature of the shock front.

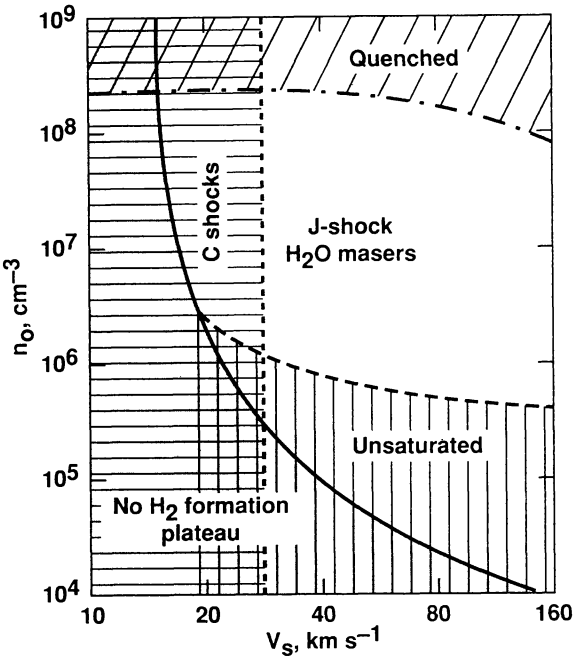

Fig. 1.— The range of preshock density n_0 and shock velocity v_s which produces strong H_2O masers (Hollenbach, Elitzur, & McKee 1995).

Shocks with velocities that exceed $\sim$ 30–40 km s^{-1} fully dissociate the gas. When the temperature drops below $\sim$ 1000 K, H_2 re-formation on the grains provides a source of heating, and the temperature stabilizes at $\sim$ 400 K until all H is transformed into H_2. This high-temperature plateau provides the favorable conditions for maser action. Shocks with lower velocities, $\sim$ 20–40 km s^{-1}, do not dissociate the material. Instead, these shocks, known as C-shocks, produce a more gradual change in physical conditions than in the case of dissociative, J-shocks. Kaufman & Neufeld (1995) have recently shown that, in spite of the difference in physical processes, the conditions behind C-shocks are generally quite similar to those behind J-shocks as far as H_2O maser generation is concerned.

Figure 1, taken from work in progress, presents the region of phase space where strong H_2O maser action occurs. For typical interstellar magnetic fields, combinations of preshock density n_0 and shock velocity v_s that fall inside the regions labeled as either J-shocks or C-shocks produce observable masers. Outside these regions, masers are either not produced or are too weak, for the technical reasons indicated. This figure may hold the key

to the dual nature of the H_2O maser phase of star formation as both widespread and selective. It shows that the phase-space for H_2O maser action is rather large, spanning a substantial range of densities and shock velocities. Strong H_2O maser emission is a robust phenomenon, generated for a wide range of physical conditions; there is no need for fine tuning of parameters. Therefore, maser action could be expected to occur at some stage of the star formation process perhaps in all sources. However, although the phase space for maser action is large, the conditions are fairly extreme. In particular, the preshock density is rather high. The dimensions of a region with such a high density probably cannot exceed $\sim 10^{17}$ cm at most. A shock with the minimal velocity of 20 km s^{-1} will move across such a small region in less than 2000 years! In observing a maser in any particular source we are witnessing a rather short lived phase. This may help explain the selectiveness of the phenomenon — although it is easy to generate an H_2O maser, that maser does not last very long.

3. WINDS, SHELLS AND JETS

Shocks seem to provide a satisfactory mechanism for H_2O maser generation in star-forming regions (e.g. Felli, Palagi, & Tofani 1992). The next problem is the construction of a scenario for the combination of powerful shocks and high densities required for maser action. A natural candidate is the high velocity outflows routinely observed in star-forming regions. When the wind from a young stellar object hits a high density clump, it drives a shock, just like those required for maser action. Some masers are undoubtedly generated this way, though issues involving clump generation and impact survival still need to be resolved.

It is important to recognize that when a highly supersonic wind is blown into a dense medium, the wind itself is quickly hidden from outside observers. Once the amount of material carried by the wind becomes comparable to the mass swept up from the ambient medium, the wind is entrapped in a dense shell. Further evolution involves the much slower motion of the shell, whose expansion is driven by the higher velocity interior wind. Simple order-of-magnitude estimates (e.g. Steigman, Strittmatter, & Williams 1975) show that the onset of the shell occurs at time and radius given by

$$t_{\rm onset} \simeq 0.7 \left(\frac{\dot{M}_{-3}}{n_{0,7} v_8^3}\right)^{1/2} \text{years}, \qquad R_{\rm onset} \simeq 2{\times}10^{15} \left(\frac{\dot{M}_{-3}}{n_{0,7} v_8}\right)^{1/2} \text{cm}. \tag{1}$$

Here $\dot{M}_{-3}$ is the wind's mass loss rate in $10^{-3} M_\odot$ yr^{-1}, v_8 is its velocity in 1000 km s^{-1}, and $n_{0,7}$ is the ambient density in 10^7 cm^{-3}. The wind parameters were normalized to values pertinent to high-mass young stellar objects, the density to typical preshock densities that produce H_2O masers. These simple estimates show that, with the parameters of the maser environment, a powerful high-velocity wind is trapped almost immediately after it turns on. In general, the wind cannot be directly observed, only the shell that it drives.

There are good indications that H_2O masers in high-mass star-forming regions trace the surfaces of shells driven by high velocity ($\sim$1000 km s^{-1}) outflows. A detailed proper motion experiment of the W49 maser source by Gwinn, Moran, & Reid (1992) reveals an intriguing velocity field with a spatial structure suggestive of an expansion from a common center. The expansion speed is almost constant, $v \approx 20$ km s^{-1}, over the range $R \approx 3{\times}10^{16}$—$10^{17}$ cm, where R is the distance from the center. At $\sim 10^{17}$ cm the v vs. R curve rises sharply and becomes nearly vertical, with the expansion speed reaching a maximum ~ 200 km s^{-1} at $R \approx 2{\times}10^{17}$ cm. If individual maser features are interpreted as gas condensations ("bullets") that move out from a common center, then each condensation must travel at a uniform speed of ~ 20 km s^{-1} throughout the interior of the region and undergo a rapid acceleration to ~ 200 km s^{-1} at its edge. This was the interpretation adopted by Gwinn et al., who also listed a number of possible mechanisms that could be responsible for the sudden acceleration at $\sim 10^{17}$ cm.

An entirely different interpretation was proposed by Mac Low & Elitzur (1992), who suggested that the masers are surface phenomena that trace the envelope of an expanding bubble. In this picture, the observed v vs. R curve implies that the shell has an elongated shape and is expanding rapidly (at a speed ~ 200 km s^{-1}) along the axis and slowly (at a speed ~ 20 km s^{-1}) perpendicular to it. Subsequent data analysis by Gwinn (1994) has verified that this model accurately reproduces the observations. His results for the rotated maser distribution viewed from perpendicular to its major axis are displayed in figure 2. The elongated distribution of features is apparent, as is the tendency of high-velocity features to lie at the periphery of the outflow, at the edge of the long axis. Mac Low & Elitzur also considered the possible dynamical origin of the observed morphology. They suggested that the elongated shell could correspond to an interstellar bubble that is driven by a high-velocity (~ 1500 km s^{-1}), spherically symmetric stellar wind that expands into a medium with an anisotropic

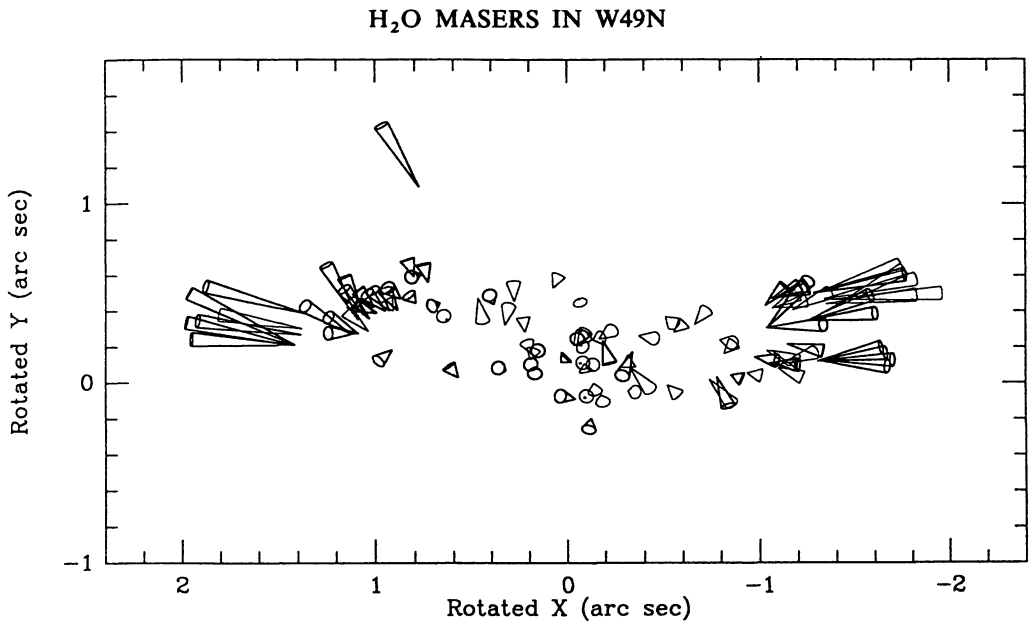

Fig. 2.— Positions and velocities of maser features in W49N, as viewed from perpendicular to the major axis of the distribution (Gwinn 1994).

density distribution. A detailed calculation showed that a spherical outflow expanding into a cylindrical cavity sweeps up the ambient gas into an elongated shell, just like the one observed. However, the postulated density distribution, with a newly formed, massive star located on the symmetry axis, was admittedly ad hoc and was used merely to illustrate the proposed new kinematic interpretation of the W49N masers in the context of a spherically symmetric stellar wind model.

While the proposal that the maser features trace the surface of an elongated shell was fully verified by the data, that of a cylindrical cavity remained unsatisfactory. In a subsequent paper Mac Low et al. (1994) proposed a more plausible origin for the elongated shell in W49N. They suggested that the outflow itself is anisotropic, specifically that it is a protostellar jet, and demonstrated that the motion of the shell of swept-up gas that is driven out by these jets can reproduce the observed v vs. R curve even when the ambient medium is isotropic. The morphology of bubbles evacuated by high-velocity jets was first analyzed by Scheuer (1974) in the context of extragalactic radio sources. He showed that the momentum transferred to the ambient medium at the jet head, where the outflow is shocked and decelerated, causes the bubble to elongate in the direction of the jet propagation. He pointed out, however, that the bubble also expands (albeit at a lower speed) in the direction normal to the jet axis on account of the high pressure of the "cocoon" of hot jet material that envelopes the jets. As was demonstrated by subsequent numerical experiments (e.g., Norman et al. 1982), the formation of an extensive cocoon requires a high-Mach-number jet whose density is lower than that of the ambient gas. In the case of protostellar jets, it is also necessary to verify that the outflow speed is high enough and its density low enough for the shocked gas not to cool before flowing out of the jet-head region (e.g., Blondin, Fryxell, & Königl 1990).

The structure of a jet cocoon is displayed in figure 3, which lists also some of the relevant expressions. In order to produce a maser shell, the outer shock must be radiative, to provide the necessary compression. The various requirements constrain the properties of the jets, and Mac Low et al. find a consistent model that produces good agreement with observations for a jet velocity $v_j \simeq 1100$ km s^{-1} and a ratio of jet density to ambient density $\rho_j/\rho_0 \simeq 0.05$. The observed ratios of the cocoon's side-to-head velocities and dimensions determine the exponent $\alpha \simeq 0$–0.23, consistent with Begelman & Cioffi (1989). The observed v vs. R curve is accurately reproduced for a cocoon age of only 320 years. This short age is unavoidable — the masers farthest from the center are at $R \sim 2\times10^{17}$ cm and have velocities of ~ 200 km s^{-1}, for a dynamical time scale of only 300 years! This extremely young age helps explain why the other objects at the core of W49 do not currently

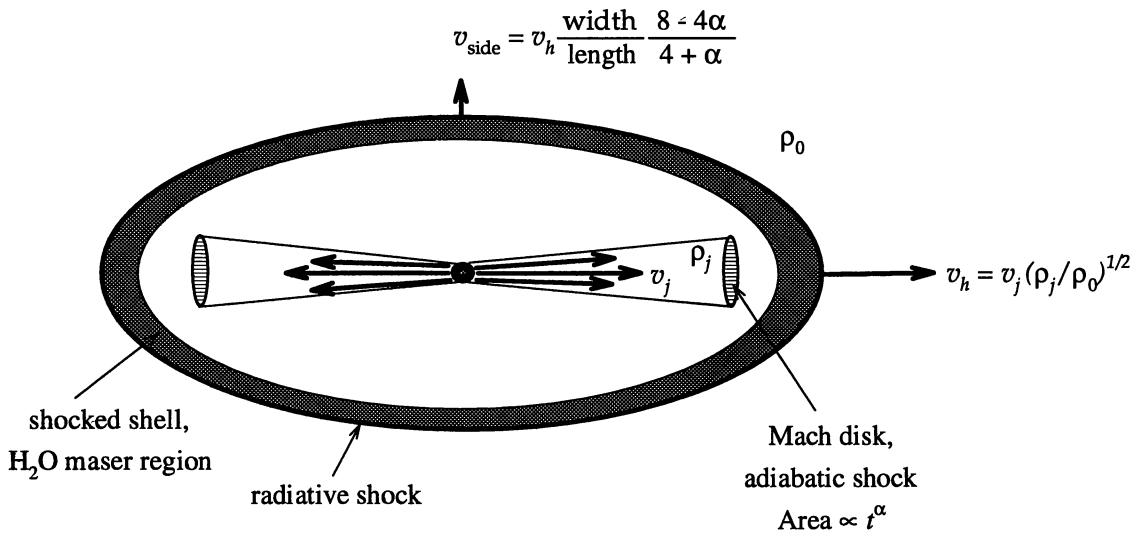

Fig. 3.— Structure of an elongated cocoon driven by twin high-velocity jets. The compressed shell at the surface of the cocoon provides the conditions required for strong H_2O maser action.

display maser emission: all of them have simply evolved past their maser phase. Indeed, Scoville et al. (1986) find that another HII region in the ring of W49 has a molecular outflow whose overall momentum is comparable to that of the maser outflow. In all likelihood, the observed molecular outflow, whose dimensions are about an order of magnitude larger, is simply a later stage (perhaps $\sim$ 10,000 years) of a maser shell. The different objects at the W49 ring provide glimpses of different stages in the evolution of a massive star.

In an exciting recent development, Reid at al. (1995) found independent evidence for a jet powering the expansion of an elongated maser shell. With VLA radio continuum observations they discovered an extremely compact synchrotron source (only $\sim 5\times10^{15}$ cm at 15 GHz), coincident with the H_2O masers in W3OH. Figure 4, taken from a proper motion study by Alcolea et al. (1992), shows a top view of the H_2O maser distribution in this source, displaying a clear bipolar structure. The synchrotron source is located at the very center of the H_2O maser distribution and displays an elongation aligned with the bipolar axis, precisely as expected if the synchrotron emission is generated by jets that also drive the expansion of a cocoon whose surface is traced by the H_2O masers. Indeed, Reid et al. point out that the most plausible source of the synchrotron emission is relativistic electrons accelerated by jet driven shocks. It is noteworthy in this regard that shock acceleration of relativistic ions was recently proposed by Ramaty, Kozlovsky, & Lingenfelter (1995) to explain COMPTEL observations of gamma ray lines in Orion.

Although a detailed v vs. R curve is not yet available for the H_2O masers in W3OH, they provide striking evidence of another jet-driven shell. Unlike W49, there are virtually no masers at the sides of this shell. The absence of such masers is immediately understood when we note that the head moves at only $v_h \sim 20$ km s^{-1}, the minimal velocity for generating masers. And since $v_{side} \ll v_h$, the W3OH shell is incapable of driving masers to its sides. Why is v_h of this shell ten times smaller than for W49? Since

$$v_h = v_j \left(\frac{n_j}{n_0}\right)^{1/2}, \qquad (2)$$

there are two possible explanations. The first one is that the jet velocity is a factor of 10 smaller, i.e., $v_j \sim 100$ km s^{-1}. This can be dismissed because such a slow jet is highly unlikely to produce the relativistic electrons required to explain the synchrotron radiation. A much more likely explanation is that the jet velocities in the two sources are comparable but the ratio n_j/n_0 in W3OH is 100 times lower, i.e., only $\sim 5\times10^{-4}$. If we further assume an ambient density of $\sim 10^7$ cm^{-3}, required for strong maser action, the jet density in W3OH is $\sim 5\times10^3$ cm^{-3}, presumably the same as its thermal electron density. From a detailed fit to the synchrotron emission, Reid et al. find that the relativistic electron density is $\sim 5\times10^{-3}$ cm^{-3}. Indeed, this combination of relativistic

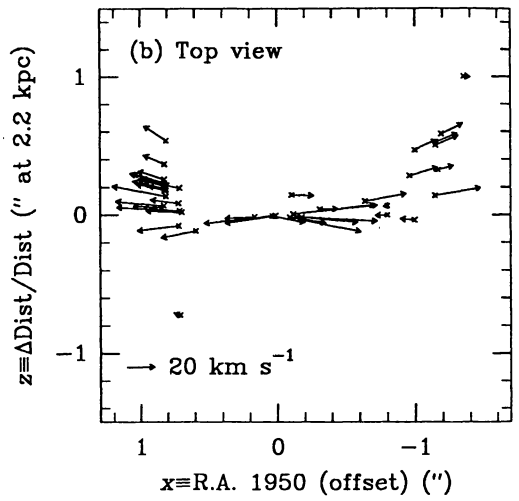

Fig. 4.— Top view of the positions and velocities of H_2O maser features in W3OH (Alcolea et al. 1992).

and thermal electron densities produces synchrotron, rather than free-free, radio emission (Garay 1995). On the other hand, the higher jet density in W49 is likely to place it in the regime of free-free dominance.

Finally, both the dimensions and axial velocity of the H_2O maser shell in W3OH are about a factor of 10 smaller than in W49 — the semi-major axis is roughly 3×10^{16} cm and it expands at about 20 km s^{-1}. Their ratio gives 500 years, again an extremely young dynamic age, comparable to that of W49.

4. SUMMARY

The observations of W49 and W3OH indicate that H_2O masers may provide the best opportunity for detailed study of jet-driven cocoons. It appears that such elongated bubbles may delineate the very last stages of formation of a high-mass star, and fine details of their structure are best probed by the masers generated on their surfaces. An intriguing possibility is that the maser morphology is controlled chiefly by n_j/n_0, the ratio of jet-to-ambient density. It is possible that W49 stands out as the most powerful Galactic maser because it is powered by the densest jet among all high-mass star-forming regions, creating bright masers over the entire bubble's surface. As the jet density decreases, the bubble's expansion velocity decreases too and the slower parts of the envelope lose their masers. In low-mass star-forming regions the ambient density can be expected to be lower and the jets penetrate without creating complete shells, leading to H-H objects and maser action only on working surfaces where they generate local shocks.

Whatever the overall structure of specific H_2O maser regions, associated short time scales seem unavoidable since they follow from direct observations of the high velocities with which maser features move and the small dimensions over which they are spread. A given maser phase cannot last more than $\sim$ 2000 years, in the concrete cases of W49 and W3OH the masers are only about 300 and 500 years old, respectively. These short time scales could possibly create problems with the statistics of star-birth rates if star formation contained just a single H_2O maser episode. Prior to the proper motion experiments, which proved that the masers indeed move at high velocities, Genzel & Downes (1977, 1979) concluded that the H_2O maser phase lasts at least 10^4 years. If this conclusion is still supported by current data, this phase would have to contain many recurring episodes of maser activity with a rather high duty cycle.

Partial support by NSF grant AST-9321847 is gratefully acknowledged.

REFERENCES

Alcolea, J., Menten, K. M., Moran, J. M., & Reid, M. J. 1992, in Astrophysical Masers, ed. A. W. Clegg & G. E. Nedoluha (Heidelberg: Springer-Verlag), 225
Begelman, M. C., & Cioffi, D. F. 1989, ApJ, 345, L21

Blondin, J. M., Fryxell, B. A., & Königl, A. 1990, ApJ, 360, 370
Elitzur, M., Hollenbach, D. J., & McKee, C. F. 1989, ApJ, 346, 983
Elitzur, M., Hollenbach, D. J., & McKee, C. F. 1992, ApJ, 394, 221
Felli, M., Palagi, F., & Tofani, G. 1992, A&A, 255, 293
Garay, G. 1995, in Disks, Outflows and Star Formation, ed. S. Lizano & J. M. Torrelles, RevMexAASC, 1, 77
Genzel, R. & Downes, D. 1977, A&AS, 30, 145.
Genzel, R. & Downes, D. 1979, A&A, 72, 234.
Gwinn, C. R. 1994, ApJ, 429, 241
Gwinn, C. R., Moran, J. M., & Reid, M. J. 1992, ApJ, 393, 149
Hollenbach, D. J., Elitzur, M., & McKee, C. F. 1995, in preparation
Kaufman, M. J., & Neufeld, D. A. 1995, ApJ, in press
Mac Low, M.-M., & Elitzur, M. 1992, ApJ, 393, L33
Mac Low, M.-M., Elitzur, M., Stone, J. M., & Königl, A. 1994, ApJ, 427, 914
Norman, M. L., Smarr, L., Winkler, K.-H. A., & Smith, M. D. 1982, A&A, 113, 285
Ramaty, R., Kozlovsky, B., & Lingenfelter, R. 1995, ApJ, in press
Reid, M. J., Argon, A. L., Masson, C. R., Menten, K. M., & Moran, J. M., 1995, ApJ, in press
Scheuer, P. A. G. 1974, MNRAS, 166, 513
Scoville et al. 1986, ApJ, 303, 416.
Steigman, G., Strittmatter, P. A. & Williams, R. E. 1975, ApJ, 198, 575
Welch, W. J., Dreher, J. W., Jackson, J. M., Tereby, S., & Vogel, S. N. 1987, Science, 238, 1550